Highly Stretchable Conductive Fibers from Few-Walled Carbon Nanotubes Coated on Poly(*m*-phenylene isophthalamide) Polymer Core/Shell Structures

Shujuan Jiang,[†,‡] Hongbo Zhang,[†] Shaoqing Song,[‡] Yanwen Ma,[†] Jinghua Li,[†] Gyeong Hee Lee,[†] Qiwei Han,[†] and Jie Liu[*,†]

[†]Department of Chemistry, Duke University, Durham, North Carolina 27708, United States and [‡]School of Chemistry, Biology and Materials Science, East China Institute of Technology, Nanchang 330013, People's Republic of China.

ABSTRACT A core/shell stretchable conductive composite of a few-walled carbon nanotube network coated on a poly(*m*-phenylene isophthalamide) fiber (FWNT/PMIA) was fabricated by a dip-coating method and an annealing process that greatly enhanced interactions between the FWNT network and PMIA core as well as within the FWNT network. The first strain–conductivity test of the as-prepared FWNT/PMIA fiber showed a stretching-induced alignment of nanotubes in the shell during the deformation process and a good conductivity stability with a slight conductivity drop from 109.63 S/cm to 98.74 S/cm ($\Delta\sigma/\sigma_0 = 10\%$) at a strain of ~150% (2.5 times the original length). More importantly, after the first stretching process, the fiber can be recovered with a slight increase in length but a greatly improved conductivity of 167.41 S/cm through an additional annealing treatment. The recovered fiber displays a similarly superb conductivity stability against stretching, with a decrease of only ~13 S/cm to 154.49 S/cm ($\Delta\sigma/\sigma_0 = 8\%$) at a strain of ~150%. We believe that this conductivity stability came from the formation and maintaining of aligned nanotube structures during the stretching process, which ensures the good tube–tube contacts and the elongation of the FWNT network without losing its conductivity. Such stable conductivity in stretchable fibers will be important for applications in stretchable electronics.

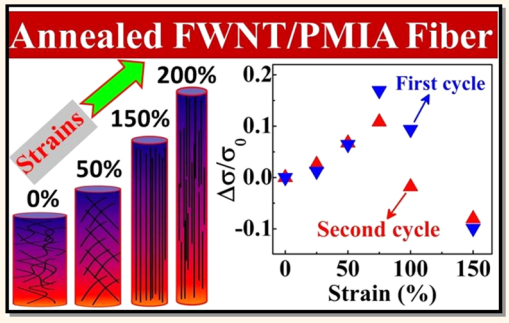

KEYWORDS: stretchable conductor · few-walled carbon nanotube · PMIA · core/shell structure · fibers · stretching-induced alignment

Stretchable conductors are highly desirable for potential applications such as flexible displays,[1−3] smart clothing,[4−6] robot parts,[7,8] transistors,[9] and energy-qrelated devices.[10−13] A suitable stretchable conductor should present three properties for these applications: (i) accommodation of high strain levels; (ii) good conductivity stability under the deformation process to maintain the operation of integrated circuits; (iii) reversibility in mechanical and electrical properties.[14] Traditional metal wires have high conductivity and stretchability, but are not reversible in mechanical property, which thus fuels the exploration for novel stretchable conductors. In general, materials designed for stretchable electronics are hybrids of an elastic substrate and an electrical conductive component, in which the former enables the reversible deformation and drives the latter to rearrange so that the conductivity can be maintained during the deformation process.[14−16] According to this mechanism, many stretchable conductive composites have been explored by using conductive materials of carbon nanotubes, metal nanostructures, or liquid metal alloys based on their excellent self-assembling capability.[16−25] However, maintaining a stable conductivity at high deformation levels especially >100% of strain, *i.e.*, the material is stretched to beyond twice the original length, is still extremely difficult to realize, mainly because of the weakened chemical bonds or reduced overlapping of electronic orbitals around the generated

* Address correspondence to j.liu@duke.edu.

Received for review July 7, 2015 and accepted September 21, 2015.

Published online September 21, 2015
10.1021/acsnano.5b04185

dislocations in the conductive components.[19] Although great effort has been devoted to resolving this inherent bottleneck that is fundamentally determined by the molecular mechanism, the conductivity–stretchability dilemma is still an unresolved problem.[24] Actually, the dislocation in the conductive component is the representation of the asynchronous deformation of the conductive component and elastic substrate or the discontinuous rearrangement of the conductive component. Therefore, the optimized structures should allow the network of the conductive components to deform synchronously with the substrate accompanied by a good self-assembling process without breakage. The former requirement can be realized by increasing the interaction between the elastomer and conductive component, while the latter requires the conductive network to maintain good electrical contacts within themselves under deformation. Thin and flexible carbon nanotube networks could be a good choice for this purpose, and a core/shell structure of a highly conductive nanotube network on an appropriate polymer substrate with an enhanced interaction between them could be an ideal system for a stretchable conductive fiber.

Aromatic polyamides, *e.g.*, poly(*m*-phenylene isophthalamide) (PMIA), as synthetic polymers possess excellent thermal and oxidative stability, flame resistance, and superior mechanical properties and, thus, have been widely used in many applications.[26,27] Herein, we developed a core/shell conductive composite from a randomly distributed few-walled carbon nanotube (FWNT) network coated on a PMIA fiber by the dip-coating method. Due to their very different thermal expansion properties, the PMIA substrate and FWNT network were partially integrated together at the contact surface by a simple annealing treatment, and also the desired tube–tube interaction was greatly enhanced. The as-fabricated novel structure showed an excellent balance of conductivity–stretchability properties as well as heat-induced mechanical and electrical reversibility, reflected by only a 10% and 8% reduction in conductivity at a strain of ~150% in the two cycles of the stretching tests.

RESULTS AND DISCUSSION

The PMIA core used here was prepared with the wet-spinning method by coagulating a PMIA dispersion in dimethylacetamide (DMAC)[28] solution, and a white PMIA fiber was obtained (S1,2 in the Supporting Information (SI)). The FWNTs[29] coated on a PMIA fiber (FWNT/PMIA) were prepared by repeatedly dipping PMIA fibers into an FWNT dispersion with Triton-X100 as the surfactant for 600 times, as shown in Figure 1A. The white PMIA fiber gradually changed to black after successively FWNT coating, and the diameter of the FWNT/PMIA fiber is thinner than a human hair

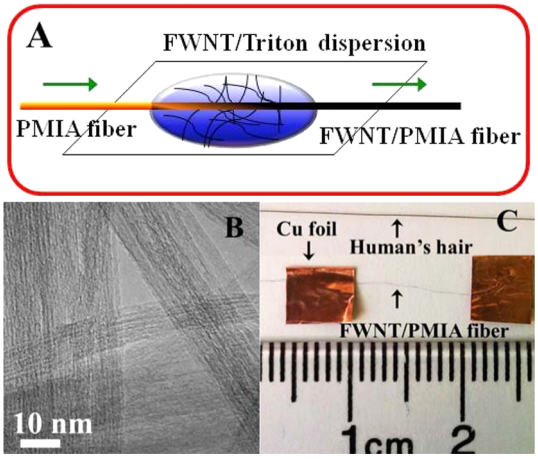

Figure 1. (A) Scheme of the preparation of the FWNT/PMIA fiber. (B) TEM image of FWNTs. (C) FWNT/PMIA fiber compared with a human hair.

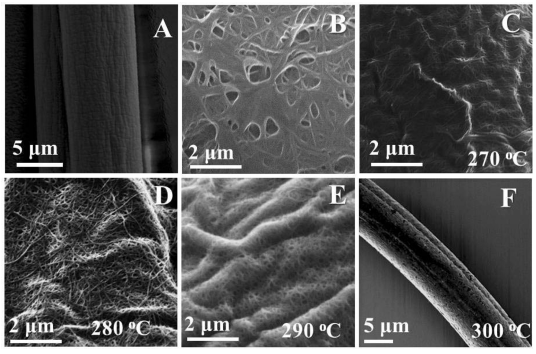

Figure 2. SEM images of PMIA and FWNT/PMIA fibers before and after annealing treatment at 270–300 °C. (A) PMIA fiber. (B–F) Unannealed FWNT/PMIA fiber (B) and its counterpart after annealing at 270 (C), 280 (D), 290 (E), and 300 °C (F).

(Figure 1C and S1 in the SI). Furthermore, the FWNT/PMIA fiber was annealed at 270, 280, 290, and 300 °C in argon in order to increase the interaction between the PMIA and FWNTs, and the corresponding samples were denoted as FWNT/PMIA-270, FWNT/PMIA-280, FWNT/PMIA-290, and FWNT/PMIA-300.

The pure PMIA fiber with an 11 ± 0.3 μm diameter has a rough surface with many tiny crisscross creases as observed by SEM (Figure 2A), and the surface of the FWNT/PMIA fiber is covered with a network of randomly distributed FWNTs (Figure 2B). On increasing the annealing temperature from 270 to 280 to 290 °C, the outline of these FWNTs becomes more and more clear due to the evaporation of the surfactant (Figure 2C–E).[30] Coupled with this process, the diameter of the composite fiber shrinks from ~12 μm to ~10 μm with progressively deeper wrinkles generated on the fiber surface, which signal the formation of an integrated layer and the enhanced interaction between PMIA and the FWNT network (S3,4 in the SI). Further increasing the annealing temperature to 300 °C causes the FWNT network to be brittle and even to peel off (Figure 2F),

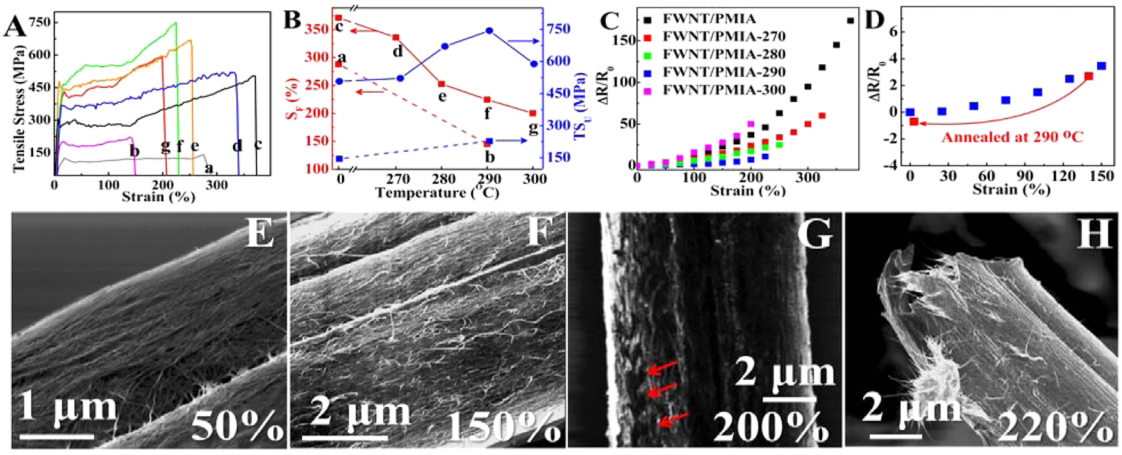

Figure 3. Mechanical and electrical properties as well as morphology evolution of the fibers under successive stretching. (A, B) Stress−strain curves for PMIA and (un)annealed FWNT/PMIA fibers (A) and their derived profile of the failure strain (S_F) and ultimate tensile stress (TS_U) as a function of annealing temperature (B). The sample in (A) and (B) corresponds to (a) PMIA, (b) PMIA-290, (c) FWNT/PMIA, (d) FWNT/PMIA-270, (e) FWNT/PMIA-280, (f) FWNT/PMIA-290, and (g) FWNT/PMIA-300. (C) Normalized resistance changes ($\Delta R/R_0$) as a function of the applied strain for (un)annealed FWNT/PMIA fibers. (D) Variation of $\Delta R/R_0$ with stretching, releasing, and recovering treatment for an FWNT/PMIA-290 fiber. (E−H) SEM images of FWNT/PMIA-290 at strains of 50%, 150%, 200%, and 220%.

possibly due to oxidation from the trace amount of oxygen in the annealing environment. This annealing treatment also causes the resistance to decrease from 80.54 (FWNT/PMIA) to 27.70 (FWNT/PMIA-270), 16.68 (FWNT/PMIA-280), 11.62 (FWNT/PMIA-290), or 12.55 kΩ/cm (FWNT/PMIA-300), which corresponds to a conductivity of 10.97, 45.99, 76.37, 109.63, and 101.50 S/cm (S5 in the SI).

To be used as stretchable conductors, the fibers should have an excellent capability of accommodating a high level of deformation without fracturing as well as no significant degradation in their electronic properties. Mechanical property analysis of the fibers shows that all the fibers demonstrated a ductile property, characterized by a well-defined yield point around ∼15% strain. The FWNT coating could improve the mechanical property of the PMIA fiber, as reflected by both the increased ultimate tensile stress (TS_U) from 147.6 MPa to 507.3 MPa and the failure strain (S_F) from 288.3% to 371.4%, which originates from the partially balanced stress and strain by the FWNTs (Figure 3A,B).[28,29] Appropriate annealing treatment can greatly improve the TS_U with a compromised S_F for FWNT/PMIA fibers. In detail, when an FWNT/PMIA fiber was annealed at 270, 280, and 290 °C, the TS_U of the FWNT/PMIA fiber was enhanced from 507.3 MPa to 521.3, 670.7, and 744.0 MPa with a S_F reduced from 371.4% to 335.9%, 252.9%, and 222.7%, respectively, which was jointly contributed by the strengthened interaction between the FWNTs and the PMIA fiber and the changed microstructure of PMIA (S2−4 in the SI).

Subsequently, the evolution of the normalized resistance change ($\Delta R/R_0$) as a function of strain was investigated for the composite fibers (Figure 3C). During the deformation process, the $\Delta R/R_0$ shows significant, different changes for the unannealed FWNT/PMIA fiber and those pretreated at 270−290 °C. At a strain of 25%, the $\Delta R/R_0$ for the unannealed FWNT/PMIA fiber is 1.5, meaning the resistance increases by 150%, and after that, a sharper increase appears in the $\Delta R/R_0$ with a value of 8.2 at 75% strain, 46.4 at 225% strain, and 174.1 at the S_F of 371.4%. This dramatic increase in $\Delta R/R_0$, however, was suppressed significantly by an appropriate annealing treatment. In detail, the values of $\Delta R/R_0$ at strains of 25%/75%/150% for FWNT/PMIA-270, FWNT/PMIA-280, and FWNT/PMIA-290 are 1.5/4.8/15.0, 1.2/3.1/15.9, and 0.06/0.9/3.4, respectively. It is notable that heat treatment at 300 °C can undermine the mechanical as well as electrical properties, as confirmed by the decreased TS_U and S_F compared to FWNT/PMIA-290 and the most significant increase in $\Delta R/R_0$ for FWNT/PMIA-300 among all the composite fibers. Therefore, the optimized fiber is FWNT/PMIA-290, with a $\Delta R/R_0$ of 11.8 at an S_F of ∼220%. The stretching test for FWNT/PMIA-290 was also recorded by video (see the SI).

Interestingly, under successive stretching, a stretching-induced alignment process in FWNTs was found by SEM observation for FWNT/PMIA-290 (Figure 3E−H). At 50% stain, the FWNTs on the ridge of the fiber have self-assembled in the parallel direction of drawing because of a larger force withstood at these areas than in the ditch. At 150% strain, all FWNTs aligned along the axial orientation. When the deformation continues to 200% strain, defective holes in the nanotube network were generated (Figure 3G). At an S_F of ∼220%, most of the FWNTs still covered the fiber in good alignment. This stretching-induced alignment process works throughout the stretching process for FWNT/PMIA-270, FWNT/PMIA-280, and FWNT/PMIA-290, compared to the formation of cracks on

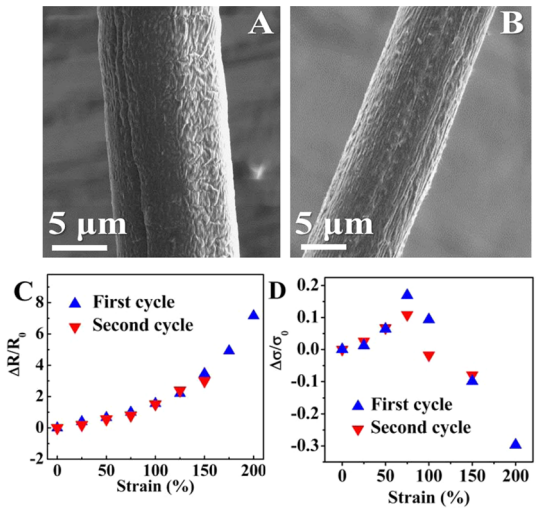

Figure 4. Morphology and electrical properties of FWNT/PMIA-290 and FWNT/PMIA-290-2. (A, B) SEM images of FWNT/PMIA-290 (A) and FWNT/PMIA-290-2 (B). (C, D) Variation of resistance ($\Delta R/R_0$) (C) and conductivity ($\Delta\sigma/\sigma_0$) (D) as a function of the strain.

the unannealed FWNT/PMIA fibers (S6 in the SI). The differences between the annealed and unannealed fibers in their morphology under stress are believed to be caused by the differences in the interactions between the FWNT shell and the PMIA core as well as between FWNTs themselves. For unannealed samples, the core and the shell are not strongly linked (S3 in the SI) and the nanotube shell does not deform together with the core. In addition, nanotubes are covered with surfactant before annealing, so the bonding between nanotubes is not strong. All of these weak interactions contributed to the formation of defects in the nanotube shells once they are stretched. The annealed samples solved these problems by increasing the interactions between the nanotube shell and the PMIA core as well as between the nanotubes within the shell (S3 in the SI).

Good mechanical and electrical reversibility are also desirable properties for stretchable conductors, and these properties for the FWNT/PMIA-290 fiber were investigated by the stretching−release test, as shown in Figure 3D. It can be seen that after releasing the fiber at a strain of 150%, the fiber can recover to a strain of ~140% by itself with the $\Delta R/R_0$ reduced from 3.4 to 2.7 (S7 in the SI). Interestingly, the FWNT/PMIA-290 fiber with 140% strain can be further recovered to a length that is only slightly longer than the original fiber (~5% strain remained) using an additional annealing treatment at 290 °C in argon. Apart from the recovered length, the resistance of the fiber was reduced from 11.62 kΩ/cm (before the test) to 7.89 kΩ/cm (S8−10 in the SI). These results confirm that the FWNT/PMIA-290 fiber has demonstrated reversibility in both deformation and conductivity originated from the enhanced interactions between the FWNT and PMIA as well as between FWNTs themselves.

The morphology and electrical stability under stress for the recovered FWNT/PMIA-290 (denoted as FWNT/PMIA-290-2) were further studied (Figure 4). It is seen that for FWNT/PMIA-290-2 the FWNT network covers the PMIA fiber tightly with many straight axial wrinkles, very different from the random ones on the original FWNT/PMIA-290, indicating the existence of alignment in the FWNTs of the shell induced by the previous stretching test (Figure 4A,B). For electrical properties, the normalized resistance and conductivity ($\Delta\sigma/\sigma_0$) changes in the two cycles have a similar tendency (Figure 4C,D) (S9 in the SI). From the variation of $\Delta\sigma/\sigma_0$, a superb electrical stability as a function of strain was found for both FWNT/PMIA-290 and FWNT/PMIA-290-2 fibers. The values of $\Delta\sigma/\sigma_0$ first increase by 17% and 12% up to a strain of 75% and then decrease by 10% and 8% at a strain of 150% for FWNT/PMIA-290 and FWNT/PMIA-290-2, respectively. This variation of conductivity with stretching was also observed in the literature, and the enhancement is explained as the contribution of the alignment of CNTs along the stretching direction.[2] For the FWNT/PMIA-290-2 sample with an aligned FWNT network, it is believed that the fiber's diameter shrinkage during the stretching test can increase the connection between the aligned nanotubes and thus improve the conductivity. Ultimately, the conductivity decreased from the original 109.63 (167.41) S/cm to 98.74 (154.49) S/cm at a strain of 150% for FWNT/PMIA-290 (FWNT/PMIA-290-2). Although the reuse capability of FWNT/PMIA-290 still needs to be improved, the good conductivity stability at the high deformation level as well as the mechanical and electrical reversibility in the two cycles are also attractive for many applications of FWNT/PMIA composite fibers in stretchable electronics. Additionally, the reusability of the core−shell structure relies on the properties of the core polymeric materials. Using an elastic core will greatly improve the number of reusable cycles.

The electrical stability of the FWNT/PMIA-290 fiber ($\Delta R/R_0$ 11.8, strain 220%) was compared with reported stretchable conductors in the literature, and the structures include films, fibers, and noble-metal-containing materials (Figure 5).[2,8,14,31−36] It can be seen that the FWNT/PMIA-290 core/shell structural fiber shows a significant improvement in the performance of the stretchable conductor with a balanced conductivity−stretchability at high deformation level. Compared with the traditional stretchable conductors based on polymer and CNT composites, the core/shell structure has overcome the tendency of disconnection between nanotubes in the composite with CNTs as conductive fillers.[17,18,31] The reason for the improved properties of this core/shell structure is the unique mechanism in avoiding the formation of dislocation in the FWNT network during stretching: the enhanced interactions between PMIA and the FWNT network as well as between FWNTs themselves enable the FWNT shell to deform

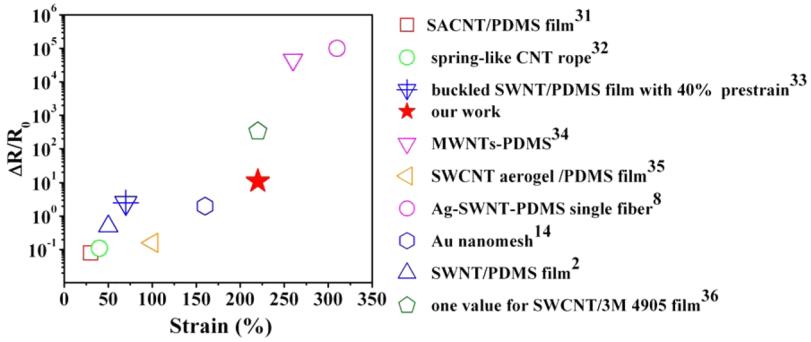

Figure 5. Comparison of the electrical stability property of FWNT/PMIA-290 with the reported stretchable conductors.

with the PMIA core and allow the self-assembling of FWNTs from a random distribution to an aligned structure. This mechanism prevents the formation of dislocations in the FWNT shell during stretching. It successfully resolved the fundamental limitation in stretchable conductors.

CONCLUSIONS

In summary, a novel core/shell stretchable conductive fiber from a FWNT network coated on PMIA was designed, and the strong interactions between the PMIA core and FWNT shell as well as between FWNTs themselves were designed and fabricated by an annealing treatment. On the basis of the enhanced interactions, the flexible FWNT network can deform synchronously with the PMIA substrate accompanied by a self-aligned process without breaking under stretching. The as-designed FWNT/PMIA fiber hence demonstrates a good balance of conductivity−stretchability and reversibility in both mechanical and electrical properties, reflected by a slight conductivity drop of 10% and 8% up to a strain of ~150% in the two cycles of the stretching tests. Therefore, the good conductivity stability at the high deformation level as well as the mechanical and electrical reversibility of FWNT/PMIA composite fibers strongly suggest their great potential in stretchable electronics and the successful strategy explored for constructing advanced stretchable conductive fibers.

METHODS

Preparation of PMIA, FWNTs, and FWNT/PMIA Fibers. PMIA fiber was prepared by a Petri-dish wet-spinning method, in which a PMIA−DMAC solution was injected from a stainless steel needle (inside diameter: ~100 μm) into a DMAC−H_2O (1:1 volume ratio) spinning solution by syringe pump at an injection rate of 0.1 mL min^{-1}. In detail, 1.2 g of PMIA (Aldrich) was dissolved in 10 mL of DMAC solution with 0.26 g of LiCl at 65 °C for 24 h, and a clear PMIA−DMAC solution was obtained. After coagulating in the spinning solution for 1 min, PMIA was drawn out, hung up to dry, and then twined for usage. The FWNT dispersion was obtained by dispersing 2.8 mg of freshly prepared FWNTs (which were synthesized as described in our previous work)[29] into 40 mL of 0.1% Triton-X100 solution by probe ultrasonication (Sonics Vibracell VC 750) for 20 min. Then the prepared PMIA fiber was dipped into the FWNT dispersion 600 times, and an FWNT layer coated on the PMIA fiber was obtained. To increase the interaction between the FWNT and PMIA, an annealing treatment was operated at 270, 280, 290, and 300 °C in an Ar atmosphere for 15 min. After the stretching test, the recovery process for the fibers adopted the same procedure with this postheating treatment. After the annealing treatment, the volume percent of the FWNT network in the FWNT/PMIA fiber was obtained to be 4.5% (S3 in the SI).

Characterization. The structure and morphology of fibers were characterized by SEM (SEM, FEI XL30). The mechanical properties of the fibers were studied using a TA Instruments RSA III microstrain analyzer. The stretching test was undertaken by a modified syringe pump as shown in S11 in the SI. The resistance of the FWNT/PMIA fibers was measured by the cyclic voltammetry method with a two-electrode model on a Biologic SP300 instrument, as well as a Keithley multimeter.

Conflict of Interest: The authors declare no competing financial interest.

Supporting Information Available: The Supporting Information is available free of charge on the ACS Publications website at DOI: 10.1021/acsnano.5b04185.

Optical images of PMIA and FWNT/PMIA fibers; mechanical properties of the PMIA fiber and its inner structure; interactions between core and shell as well as between tube−tube in the shell; inner structures of FWNT/PMIA fibers; resistance and conductivity of the FWNT/PMIA fibers; SEM images of the fibers after the stretching test and recovering treatment; stress−strain curves in the stretching−releasing test; mechanical and electrical reversibility of the FWNT/PMIA-290 fiber; resistance and diameter changes as a function of the strain; mechanical and electrical properties as a function of curing time and reuse capability; the equipment used for resistance−strain tests (PDF)

Acknowledgment. This work is in-part supported by grants from NSF (EECS-1344745) and NSF (CHE-1213469). The authors also acknowledge the support from Duke University SMIF (Shared Materials Instrumentation Facilities). S.J. acknowledges support from the China Scholarship Council for a one-year postdoctoral fellowship that enabled her visit to Duke University.

REFERENCES AND NOTES

1. Park, S. I.; Xiong, Y. J.; Kim, R. H.; Elvikis, P.; Meitl, M.; Kim, D. H.; Wu, J.; Yoon, J.; Yu, C. J.; Liu, Z. J.; et al. Printed Assemblies of Inorganic Light-Emitting Diodes for Deformable and Semitransparent Displays. *Science* **2009**, *325*, 977–981.
2. Yu, Z. B.; Niu, X. F.; Liu, Z. T.; Pei, Q. B. Intrinsically stretchable polymer light-Emitting Devices Using Carbon Nanotube-Polymer Composite Electrodes. *Adv. Mater.* **2011**, *23*, 3989–3994.

3. Sekitani, T.; Nakajima, H.; Maeda, H.; Fukushima, T.; Aida, T.; Hata, K.; Someya, T. Stretchable Active-Matrix Organic Light-Emitting Diode Display Using Printable Elastic Conductors. *Nat. Mater.* **2009**, *8*, 494–499.
4. Service, R. F. Electronic Textiles Charge Ahead. *Science* **2003**, *301*, 909–911.
5. Kim, K. N.; Chun, J.; Kim, J. W.; Lee, K. Y.; Park, J. U.; Kim, S. W.; Wang, Z. L.; Baik, J. M. Highly Stretchable 2D Fabrics for Wearable Triboelectric Nanogenerator under Harsh Environments. *ACS Nano* **2015**, *9*, 6394–6400.
6. Choi, S.; Park, J.; Hyun, W.; Kim, J.; Kim, J.; Lee, Y. B.; Song, C.; Hwang, H. J.; Kim, J. H.; Hyeon, T.; et al. Stretchable Heater Using Ligand-Exchanged Silver Nanowire Nanocomposite for Wearable Articular Thermotherapy. *ACS Nano* **2015**, *9*, 6626–6633.
7. Sekitani, T.; Noguchi, Y.; Hata, K.; Fukushima, T.; Aida, T.; Someya, T. A Rubberlike Stretchable Active Matrix Using Elastic Conductors. *Science* **2008**, *321*, 1468–1472.
8. Ma, R. J.; Lee, J. Y.; Choi, D. M.; Moon, H.; Baik, S. Knitted Fabrics Made from Highly Conductive Stretchable Fibers. *Nano Lett.* **2014**, *14*, 1944–1951.
9. Chortos, A.; Lim, J.; To, J. W. F.; Vosgueritchian, M.; Dusseault, T. J.; Kim, T. H.; Hwang, S.; Bao, Z. N. Highly Stretchable Transistors Using A Microcracked Organic Semiconductor. *Adv. Mater.* **2014**, *26*, 4253–4259.
10. Zhang, Z. T.; Yang, Z. B.; Deng, J.; Zhang, Y.; Guan, G. Z.; Peng, H. S. Stretchable Organic Solar Cell. *Small* **2015**, *11*, 675–680.
11. Hu, L. B.; Pasta, M.; Mantia, F. L.; Cui, L. F.; Jeong, S.; Deshazer, H. D.; Choi, J. W.; Han, S. M.; Cui, Y. Stretchable, Porous and Conductive Energy Textiles. *Nano Lett.* **2010**, *10*, 708–714.
12. Xie, K. Y.; Wei, B. Q. Materials and Structures for Stretchable Energy Storage and Conversion Devices. *Adv. Mater.* **2014**, *26*, 3592–3617.
13. Zhou, G. M.; Li, F.; Cheng, H. M. Progress in Flexible Lithium Batteries and Future Prospects. *Energy Environ. Sci.* **2014**, *7*, 1307–1338.
14. Guo, C. F.; Sun, T. Y.; Liu, Q. H.; Suo, Z. G.; Ren, Z. F. Highly Stretchable and Transparent Nanomesh Electrodes Made by Grain Boundary Lithography. *Nat. Commun.* **2014**, *5*, 1–8.
15. Suo, Z. G. Mechanics of Stretchable Electronics and Soft Machines. *MRS Bull.* **2012**, *37*, 218–225.
16. Yao, S. S.; Zhu, Y. Nanomaterial-Enabled Stretchable Conductors: Strategies, Materials and Devices. *Adv. Mater.* **2015**, *27*, 1480–1511.
17. Lipomi, D. J.; Vosgueritchian, M.; Tee, B. C. K.; Hellstrom, S. L.; Lee, J. A.; Fox, C. H.; Bao, Z. N. Skin-Like Pressure and Strain Sensors Based on Transparent Elastic Films of Carbon Nanotubes. *Nat. Nanotechnol.* **2011**, *6*, 788–792.
18. Chun, K. Y.; Oh, Y.; Rho, J.; Ahn, J. H.; Kim, Y. J.; Choi, H. R.; Baik, S. Highly Conductive, Printable and Stretchable Composite Films of Carbon Nanotubes and Silver. *Nat. Nanotechnol.* **2010**, *5*, 853–857.
19. Kim, Y.; Zhu, J.; Yeom, B.; Di Prima, M.; Su, X. L.; Kim, J. G.; Yoo, S. J.; Uher, C.; Kotov, N. A. Stretchable Nanoparticle Conductors with Self-Organized Conductive Pathways. *Nature* **2013**, *500*, 59–63.
20. Yamada, T.; Hayamizu, Y.; Yamamoto, Y.; Yomogida, Y.; Izadi-Najafabadi, A.; Futaba, D. N.; Hata, K. A Stretchable Carbon Nanotube Strain Sensor for Human-Motion Detection. *Nat. Nanotechnol.* **2011**, *6*, 296–301.
21. Ahn, B. Y.; Duoss, E. B.; Motala, M. J.; Guo, X. Y.; Park, S. I.; Xiong, Y. J.; Yoon, J.; Nuzzo, R. G.; Rogers, J. A.; Lewis, J. A. Omnidirectional Printing of Flexible, Stretchable, and Spanning Silver Microelectrodes. *Science* **2009**, *323*, 1590–1593.
22. Zhu, Y.; Xu, F. Buckling of Aligned Carbon Nanotubes as Stretchable Conductors: A New Manufacturing Strategy. *Adv. Mater.* **2012**, *24*, 1073–1077.
23. Fassler, A.; Majidi, C. Liquid-Phase Metal Inclusions for a Conductive Polymer Composite. *Adv. Mater.* **2015**, *27*, 1928–1932.
24. Park, M.; Im, J.; Shin, M.; Min, Y.; Park, J.; Cho, H.; Park, S.; Shim, M. B.; Jeon, S.; Chung, D. Y.; et al. Highly Stretchable Electric Circuits From A Composite Material of Silver Nanoparticles and Elastomeric Fibres. *Nat. Nanotechnol.* **2012**, *7*, 803–809.
25. Vural, M.; Behrens, A. M.; Ayyub, O. B.; Ayoub, J. J.; Kofinas, P. Sprayable Elastic Conductors Based on Block Copolymer Silver Nanoparticle Composites. *ACS Nano* **2015**, *9*, 336–344.
26. Jeong, Y. G.; Jeon, G. W. Microstruture and Performance of Multiwalled Carbon Nanotube/m-Aramid Composite Films as Electric Heating Elements. *ACS Appl. Mater. Interfaces* **2013**, *5*, 6527–6534.
27. Gabara, V.; Hartzler, J. D.; Lee, K.-S.; Rodini, D. J.; Yang, H. H. Aramid fibers. In *Handbook of Fiber Chemistry*, 3rd ed.; Lewin, M., Ed.; CRC Press: Boca Raton, FL, 2007.
28. Wang, X. R.; Si, Y.; Wang, X. F.; Yang, J. M.; Ding, B.; Chen, L.; Hu, Z. M.; Yu, J. Y. Tuning Hierarchically Aligned Structures for High-Strength PMIA-MWCNT Hybrid Nanofibers. *Nanoscale* **2013**, *5*, 886–889.
29. Hou, Y.; Tang, J.; Zhang, H. B.; Qian, C.; Feng, Y. Y.; Liu, J. Functionalized Few-Walled Carbon Nanotubes for Mechanical Reinforcement of Polymeric Composites. *ACS Nano* **2009**, *3*, 1057–1062.
30. Mitsuda, K.; Kimura, H.; Murahashi, T. Evaporation and Decomposition of Triton X-100 under Various Gases and Temperatures. *J. Mater. Sci.* **1989**, *24*, 413–419.
31. Liu, K.; Sun, Y. H.; Liu, P.; Lin, X. Y.; Fan, S. S.; Jiang, K. L. Cross-Stacked Super Aligned Carbon Nanotube Films for Transparent and Stretchable Conductors. *Adv. Funct. Mater.* **2011**, *21*, 2721–2728.
32. Shang, Y. Y.; He, X. D.; Li, Y. B.; Zhang, L. H.; Li, Z.; Ji, C. Y.; Shi, E. Z.; Li, P. X.; Zhu, K.; Peng, Q. Y.; et al. Super-Stretchable Spring-Like Carbon Nanotube Ropes. *Adv. Mater.* **2012**, *24*, 2896–2900.
33. Yu, C. J.; Masarapu, C.; Rong, J. P.; Wei, B. Q.; Jiang, H. Q. Stretchable Supercapacitors Based on Buckled Single-Walled Carbon Nanotube Macrofilms. *Adv. Mater.* **2009**, *21*, 4793–4797.
34. Huang, Y. Y.; Terentjev, E. M. Tailoring the Electrical Properties of Carbon Nanotube-Polymer Composites. *Adv. Funct. Mater.* **2010**, *20*, 4062–4068.
35. Kim, K. H.; Vural, M.; Islam, M. F. Single-Walled Carbon Nanotube Aerogel-Based Elastic Conductors. *Adv. Mater.* **2011**, *23*, 2865–2869.
36. Kim, T.; Song, H.; Ha, J.; Kim, S.; Kim, D.; Chung, S.; Lee, J.; Hong, Y. Inkjet-Printed Stretchable Single-Walled Carbon Nanotube Electrodes with Excellent Mechanical Properties. *Appl. Phys. Lett.* **2014**, *104*, 113103.